COMMUNICATIONS IN NUMERICAL METHODS IN ENGINEERING
Commun. Numer. Meth. Engng 2000; **16**:439–448

The θ scheme for time-domain BEM/FEM coupling applied to the 2-D scalar wave equation

W. J. Mansur[1,*], Guoyou Yu[2], J. A. M. Carrer[1], S. T. Lie[3] and E. F. N. Siqueira[1]

Civil Engineering Department, COPPE-Federal University of Rio de Janeiro, Caixa Postal 68506, CEP 21945-970, Rio de Janeiro, RJ, Brazil
[2] *Ocean Engineering Department of Tianjin University, Tianjin, 300072, People's Republic of China*
[3] *School of Civil and Structural Engineering, Nanyang Technological University, Nanyang Avenue, Singapore 639798, Singapore*

SUMMARY

There exist quite a number of published papers showing that BEM/FEM coupling in time domain is a robust procedure leading to great computer time savings for infinite domain analyses. However, in many cases, the procedures presented so far have considered only constant time interpolation for BEM tractions, otherwise one may have (mainly in bounded domains) strong oscillations which invalidate the results. In this paper, such a limitation is overcome by employing the linear θ method which consists, basically, of computing the response at the time t_{n+1} from the response previously computed at the time $t_{n+\theta}$, $\theta \geqslant 1.0$. This procedure is implicitly incorporated into the BEM algorithm in the coupled BEM/FEM process presented here, i.e. the response is calculated directly at time t_{n+1}. Proceeding this way, it becomes possible to adopt the Newmark scheme in the FEM algorithm. Two examples are presented in order to validate the formulation. Copyright © 2000 John Wiley & Sons, Ltd.

KEY WORDS: linear θ method; BEM/FEM coupling; scalar wave equation; acoustics

INTRODUCTION

The purpose of this work is the presentation of a new BEM/FEM coupling procedure for scalar wave propagation analysis in the time domain. The FEM employs the Newmark time-marching scheme [1, 2] whereas for the BEM a time-domain formulation which makes use of linear time interpolation functions for the flux is employed. This BEM approach is known as linear θ method and was presented by Yu *et al.* [3] in order to overcome the difficulty of the standard time-domain BEM formulation [4–7] to perform closed domain analysis by assuming a

* Correspondence to: W. J. Mansur, Department of Civil Engineering, COPPE/UFRJ, Cidade Universitaria, CT, Bloco B, Sala 100, Caixa Postal 68506, CEP 21945-970, Rio de Janeiro, RJ, Brazil

Contract/grant sponsor: CNPq; contract/grant number 301104/95-6 (NV) and 300210/92-2 (RN)
Contract/grant sponsor: PRONEX/MCT

Received 24 May 1999
Accepted 3 December 1999

linear-time approximation for the flux. In fact, since 1983, when Mansur [7] established the general time-domain BEM formulation for the scalar wave equation and elastodynamics, constant time interpolation was considered as the only way to take into account the flux time discontinuities that occur in closed domain analyses. Since then, alternative schemes have appeared in the literature in order to make possible the use of linear time interpolation functions for the flux, e.g., Yu *et al.* [3] and Mansur *et al.* [8].

The linear θ method [3] considers flux and potential to vary linearly from time t to time $t + \theta\Delta t (\theta \geqslant 1.0)$. The method is not unconditionally stable; however, as shown by Yu *et al.* [3], it is stable for any realistic time-step choice.

Two examples are presented in this paper. The numerical results can be considered fairly good, letting one to conclude that the BEM/FEM coupling procedure is reliable for bounded and unbounded time-domain analyses. The second example shows the advantage of coupling procedures: the region of interest can be discretized with finite elements and the boundary elements play the role of an absorbing boundary.

THE LINEAR θ METHOD FOR THE BEM

The numerical procedure referred to as standard here is that presented by Mansur [7] and by Mansur and Carrer [9].

In the linear θ method [3], a different last time step $[t_n, t_{n+\theta}]$ is used, instead of $[t_n, t_{n+1}]$, where $t_{n+\theta} = t_n + \theta\Delta t$, $\theta \geqslant 1$. Responses at time t_{n+1} can be computed from responses at $t_{n+\theta}$ by following the relationship below:

$$u_i^{n+1} = \frac{1}{\theta} u_i^{n+\theta} + \frac{\theta - 1}{\theta} u_i^n, \quad p_i^{n+1} = \frac{1}{\theta} p_i^{n+\theta} + \frac{\theta - 1}{\theta} p_i^n \tag{1}$$

Unknowns $u_i^{n+\theta}$ and $p_i^{n+\theta}$ can be computed from the following equation [3]:

$$4\pi c(S_i)\, u_i^{n+\theta} + \sum_{j=1}^{J} H_{ij}^{(n+\theta)(n+\theta)} u_j^{n+\theta} - \sum_{j=1}^{J} G_{ij}^{(n+\theta)(n+\theta)} p_j^{n+\theta} = \sum_{m=1}^{n} \sum_{j=1}^{J} G_{ij}^{(n+\theta)m} p_j^m - \sum_{m=1}^{n} \sum_{j=1}^{J} H_{ij}^{(n+\theta)m} u_j^m \tag{2}$$

where:

$$H_{ij}^{(n+\theta)m} = -\int_\Gamma \frac{\partial r(S_i, Q)}{\partial n(Q)} \eta_j(Q) \int_0^{t_{n+\theta}} [\phi_u^m(\tau)\, B^*(Q, t_{n+\theta}; S_i, \tau) + \frac{1}{c} \frac{d\phi_u^m(\tau)}{d\tau} u^*(Q, t_{n+\theta}; S_i, \tau)]\, d\tau\, d\Gamma(Q) \tag{3}$$

$$G_{ij}^{(n+\theta)m} = \int_\Gamma \gamma_j(Q) \int_0^{t_{n+\theta}} \phi_p^m(\tau) u^*(Q, t_{n+\theta}; S_i, \tau)\, d\tau\, d\Gamma(Q)$$

and

$$H_{ij}^{(n+\theta)(n+\theta)} = -\int_\Gamma \frac{\partial r(S_i, Q)}{\partial n(Q)} \eta_j(Q) \int_0^{t_{n+\theta}} [\phi_u^{n+\theta}(\tau)\, B^*(Q, t_{n+\theta}; S_i, \tau) + \frac{1}{c} \frac{\mathrm{d}\phi_u^{n+\theta}(\tau)}{\mathrm{d}\tau} u^*(Q, t_{n+\theta}; S_i, \tau)]\, \mathrm{d}\tau \mathrm{d}\Gamma(Q) \tag{4}$$

$$G_{ij}^{(n+\theta)(n+\theta)} = \int_\Gamma \gamma_j(Q) \int_0^{t_{n+\theta}} \phi_p^{n+\theta}(\tau)\, u^*(Q, t_{n+\theta}; S_i, \tau)\, \mathrm{d}\tau\, \mathrm{d}\Gamma(Q)$$

Expressions for the fundamental solution $u^*(Q, t; S, \tau)$, and for $\mathrm{B}^*(Q, t; S, \tau)$ can be found in References [3, 7].

In order to couple the BEM with FEM equations originated from the Newmark method [1, 2], the procedure described so far has to be modified in such a way that u^{n+1} and p^{n+1} appear explicitly, instead of $u^{n+\theta}$ and $p^{n+\theta}$ in Equation (2). The followed procedure is described next.

From Equation (1) one can write

$$u_i^{n+\theta} = \theta u_i^{n+1} - (\theta - 1) u_i^n;\ p_i^{n+\theta} = \theta p_i^{n+1} - (\theta - 1) p_i^n \tag{5}$$

Substitution of Equations (5) into Equation (2) gives

$$\begin{aligned} &\theta \left[4\pi c(S_i) + \sum_{j=1}^{J} H_{ij}^{(n+\theta)(n+\theta)} \right] u_j^{n+1} - \theta \sum_{j=1}^{J} G_{ij}^{(n+\theta)(n+\theta)} p_j^{n+1} \\ &\quad = (\theta - 1) \left\{ \left[4\pi c(S_i) + \sum_{j=1}^{J} H_{ij}^{(n+\theta)(n+\theta)} \right] u_j^n - \sum_{j=1}^{J} G_{ij}^{(n+\theta)(n+\theta)} p_j^n \right\} \\ &\qquad + \sum_{m=1}^{n} \sum_{j=1}^{J} G_{ij}^{(n+\theta)m} p_j^m - \sum_{m=1}^{n} \sum_{j=1}^{J} H_{ij}^{(n+\theta)m} u_j^m \end{aligned} \tag{6}$$

Equation (6) can be written in matrix form as:

$$\theta(\mathbf{C} + \mathbf{H}(\theta))\, \mathbf{u}^{n+1} - \theta \mathbf{G}(\theta)\, \mathbf{p}^{n+1} = \mathbf{r}^n \tag{7}$$

After considering the prescribed boundary conditions, the following equation arises:

$$\mathbf{A}\mathbf{x}^{n+1} = \mathbf{B}\mathbf{y}^{n+1} + \mathbf{r}^n \tag{8}$$

where:

$$\mathbf{r}^n = (\theta - 1)[(\mathbf{C} + \mathbf{H}(\theta))\mathbf{u}^n - \mathbf{G}(\theta)\, \mathbf{p}^n] + \sum_{m=1}^{n} \mathbf{G}(\theta)^{n-m+1}\, \mathbf{p}^m - \sum_{m=1}^{n} \mathbf{H}(\theta)^{n-m+1} \mathbf{u}^m \tag{9}$$

Boundary unknowns at time t_{n+1} can be computed from Equation (8), which can also be used in a coupled BEM/FEM procedure in the same way usually employed for the standard BEM formulation as will be discussed in the following sections.

It can be seen that if $\theta = 1$, Equation (8) becomes the standard BEM equation [7]. If $\theta \geqslant 1$, the present formulation, however, is stable when linear flux time interpolation functions are employed, whereas the standard one fails in closed domain analyses.

NEWMARK ALGORITHM FOR THE FEM

The Newmark scheme [1, 2], for $\alpha = 1/4$ and for $\delta = 1/2$ leads to the following version of the FEM dynamic equilibrium equations for an undamped system ($\bar{\mathbf{K}} = \mathbf{K}_{\text{eff}}$; $\bar{\mathbf{R}}^{n+1} = \mathbf{R}_{\text{eff}}^{n+1}$)

$$\bar{\mathbf{K}}\mathbf{u}^{n+1} = \bar{\mathbf{R}}^{n+1} \tag{10}$$

where:

$$\bar{\mathbf{K}} = \frac{4}{\Delta t^2}\mathbf{M} + \mathbf{K}, \quad \bar{\mathbf{R}}^{n+1} = \mathbf{R}^n + \mathbf{M}\left(\frac{4}{\Delta t^2}\mathbf{u}^n + \frac{4}{\Delta t}\dot{\mathbf{u}}^n + \ddot{\mathbf{u}}^n\right) \tag{11}$$

BEM/FEM COUPLING PROCEDURE

In order to develop the coupling procedure, consider first the Ω domain of a continuous medium subdivided into two sub-domains Ω_{BE} and Ω_{FE} ($\Omega = \Omega_{\text{BE}} \cup \Omega_{\text{FE}}$) with a common interface Γ_i. The sub-domain Ω_{BE} is modelled by boundary elements and the sub-domain Ω_{FE} by finite elements (see Figure 1).

The notation employed in the following developments considers that the subscript 'o' is associated to nodes that do not belong to Γ_i and the subscript 'i' is associated to nodes that belong

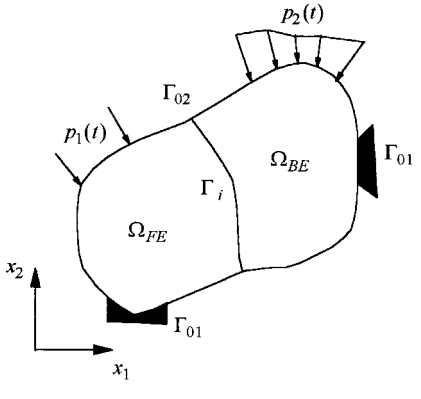

Figure 1. General representation of Ω_{FE} and Ω_{BE} sub-domains.

to Γ_i, whereas the subscript F refers to the subdomain Ω_{FE}, and the subscript B refers to the subdomain Ω_{BE}. Thus, on Γ_i the *equilibrium condition* reads $\mathbf{p}_{Fi}(s,t) = -\mathbf{p}_{Bi}(s,t)$ and the *compatibility condition* reads $\mathbf{u}_{Fi}(s,t) = \mathbf{u}_{Bi}(s,t)$.

In order to establish the coupling algorithm, the BEM system of equations must be written for the subdomain Ω_{BE}, and organized in such a way that all entries of the vector $\mathbf{x}^{n+1}$ in Equation (8), concerning nodes located at Γ_i, remains in a subvector $\mathbf{x}_{Bi}^{n+1}$ which contains unknown nodal interface fluxes. Consequently, all entries of $\mathbf{x}^{n+1}$ not related to Γ_i will remain in another subvector $\mathbf{x}_{Bo}^{n+1}$, $\mathbf{x}^{n+1} = \mathbf{x}_{Bi}^{n+1} \cup \mathbf{x}_{Bo}^{n+1}$. Thus, matrices $\mathbf{A}$ and $\mathbf{B}$ in Equation (8) are composed of four submatrices each, respectively denoted $\mathbf{A}_{jk}$ and $\mathbf{B}_{jk}$, $j, k = \mathrm{i}, \mathrm{o}$, and vectors $\mathbf{y}^{n+1}$ and $\mathbf{r}^n$ are composed of two subvectors each, respectively denoted $\mathbf{y}_{Bk}^{n+1}$ and $\mathbf{r}_{Bk}^n$, $k = \mathrm{i}, \mathrm{o}$. It should be observed that $\mathbf{y}_{Bi}^{n+1} = \mathbf{u}_{Bi}^{n+1}$.

Thus, Equation (8) for the subdomain Ω_{BE} can be written as

$$\begin{Bmatrix} \mathbf{x}_{Bo}^{n+1} \\ \mathbf{p}_{Bi}^{n+1} \end{Bmatrix} = \begin{bmatrix} \mathbf{Q}_{oo}(\mathbf{B}_{oo}\mathbf{y}_{Bo}^{n+1} + \mathbf{r}_{Bo}^n) + \mathbf{Q}_{oi}(\mathbf{B}_{io}\mathbf{y}_{Bo}^{n+1} + \mathbf{r}_{Bi}^n) + (\mathbf{Q}_{oo}\mathbf{B}_{oi} + \mathbf{Q}_{oi}\mathbf{B}_{ii})\mathbf{u}_{Bi}^{n+1} \\ \mathbf{Q}_{io}(\mathbf{B}_{oo}\mathbf{y}_{Bo}^{n+1} + \mathbf{r}_{Bo}^n) + \mathbf{Q}_{ii}(\mathbf{B}_{io}\mathbf{y}_{Bo}^{n+1} + \mathbf{r}_{Bi}^n) + (\mathbf{Q}_{io}\mathbf{B}_{oi} + \mathbf{Q}_{ii}\mathbf{B}_{ii})\mathbf{u}_{Bi}^{n+1} \end{bmatrix} \tag{12}$$

where

$$\begin{bmatrix} \mathbf{Q}_{oo} & \mathbf{Q}_{oi} \\ \mathbf{Q}_{io} & \mathbf{Q}_{ii} \end{bmatrix} = \begin{bmatrix} \mathbf{A}_{oo} & \mathbf{A}_{oi} \\ \mathbf{A}_{io} & \mathbf{A}_{ii} \end{bmatrix}^{-1} \tag{13}$$

By considering the equilibrium condition at the interface ($\mathbf{p}_{Fi}(s,t) = -\mathbf{p}_{Bi}(s,t)$), the following expression can be written, [1, 2]:

$$\mathbf{R}_{Fi}^{n+1} = \sum_{e=1}^{nfei} \int_{\Gamma_e} \mathbf{H}^{\Gamma_e} \mathbf{p}_{Fi}(s, t_{n+1})\, d\Gamma = \left(\sum_{e=1}^{nfei} \int_{\Gamma_e} \mathbf{H}^{\Gamma_e} \gamma\, d\Gamma \right) \mathbf{p}_{Fi}^{n+1} = \mathbf{F}\mathbf{p}_{Fi}^{n+1} = -\mathbf{F}\mathbf{p}_{Bi}^{n+1} \tag{14}$$

By considering the compatibility condition ($\mathbf{u}_{Fi}(s,t) = \mathbf{u}_{Bi}(s,t)$) in Equation (12) and then substituting the resulting expression for $\{\mathbf{p}_{Bi}^{n+1}\}$ into Equation (14), one has

$$\mathbf{R}_{Fi}^{n+1} = -\mathbf{F}[\mathbf{Q}_{io}(\mathbf{B}_{oo}\mathbf{y}_{Bo}^{n+1} + \mathbf{r}_{Bo}^n) + \mathbf{Q}_{ii}(\mathbf{B}_{io}\mathbf{y}_{Bo}^{n+1} + \mathbf{r}_{Bi}^n)] - \mathbf{F}[\mathbf{Q}_{io}\mathbf{B}_{oi} + \mathbf{Q}_{ii}\mathbf{B}_{ii}]\mathbf{u}_{Fi}^{n+1} \tag{15}$$

A similar procedure must now be followed for the subdomain Ω_{FE}. From Equation (10), submatrices $\bar{\mathbf{K}}_{jk}$, $j, k = \mathrm{i}, \mathrm{o}$ and vectors $\mathbf{u}_{Fk}^{n+1}$ and $\bar{\mathbf{R}}_{Fk}^{n+1}$ $k = \mathrm{i}, \mathrm{o}$ are generated.

When expression (15) is substituted into Equation (10), organized as described above, the FEM system can be written as:

$$\begin{bmatrix} \bar{\mathbf{K}}_{oo} & \bar{\mathbf{K}}_{oi} \\ \bar{\mathbf{K}}_{io} & \bar{\mathbf{K}}_{ii} + \mathbf{F}(\mathbf{Q}_{io}\mathbf{B}_{oi} + \mathbf{Q}_{ii}\mathbf{B}_{ii}) \end{bmatrix} \begin{Bmatrix} \mathbf{u}_{Fo}^{n+1} \\ \mathbf{u}_{Fi}^{n+1} \end{Bmatrix} = \begin{Bmatrix} \bar{\mathbf{R}}_{Fo}^{n+1} \\ \bar{\mathbf{f}}_{Fi}^{n+1} \end{Bmatrix} \tag{16}$$

where

$$\bar{\mathbf{f}}_{\mathrm{Fi}}^{n+1} = (\mathbf{M}_{\mathrm{io}}\mathbf{r}_{\mathrm{Fo}}^{n} + \mathbf{M}_{\mathrm{ii}}\mathbf{r}_{\mathrm{Fi}}^{n}) - \mathbf{F}\left[\mathbf{Q}_{\mathrm{io}}(\mathbf{B}_{\mathrm{oo}}\mathbf{y}_{\mathrm{Bo}}^{n+1} + \mathbf{r}_{\mathrm{Bo}}^{n}) + \mathbf{Q}_{\mathrm{ii}}(\mathbf{B}_{\mathrm{io}}\mathbf{y}_{\mathrm{Bo}}^{n+1} + \mathbf{r}_{\mathrm{Bi}}^{n})\right] \tag{17}$$

and:

$$\begin{Bmatrix} \mathbf{r}_{\mathrm{Fo}}^{n} \\ \mathbf{r}_{\mathrm{Fi}}^{n} \end{Bmatrix} = \begin{bmatrix} \dfrac{1}{\Delta t^2}\mathbf{u}_{\mathrm{Fo}}^{n} + \dfrac{1}{\Delta t}\dot{\mathbf{u}}_{\mathrm{Fo}}^{n} + \ddot{\mathbf{u}}_{\mathrm{Fo}}^{n} \\ \dfrac{1}{\Delta t^2}\mathbf{u}_{\mathrm{Fi}}^{n} + \dfrac{1}{\Delta t}\dot{\mathbf{u}}_{\mathrm{Fi}}^{n} + \ddot{\mathbf{u}}_{\mathrm{Fi}}^{n} \end{bmatrix} \tag{18}$$

Displacements in the FEM sub-domain can be obtained by solving Equation (16). Other quantities such as velocities, accelerations, support reactions, stresses, etc., in that sub-domain can determined following standard FEM procedures. By observing that $\mathbf{u}_{\mathrm{Bi}}^{n+1} = \mathbf{u}_{\mathrm{Fi}}^{n+1}$, it is also possible to calculate, by means of Equation (12), the boundary unknowns in the region discretized with boundary elements, and then the internal points state variables.

NUMERICAL EXAMPLES

Waveguide

The example depicted in Figure 2, previously presented by Mansur [7], has been chosen to be analysed here because it is prone to severe numerical instabilities and illustrates quite well the stability improvement that arises from using the linear θ method described in this paper. It consists of a waveguide subjected to a Heaviside-type flux forcing function applied at one extremity (see Figure 2). Isoparametric linear FE were used for half of the domain, the other half

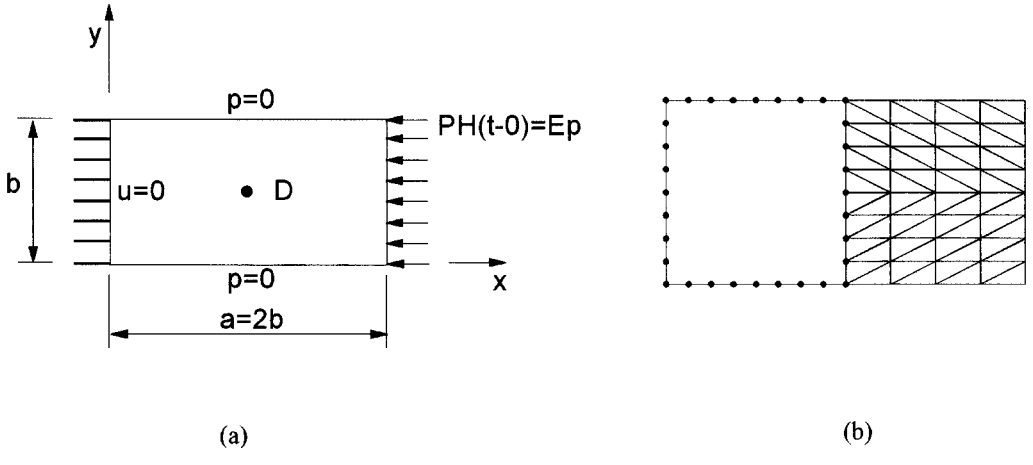

Figure 2. Waveguide under a Heaviside-type forcing function.

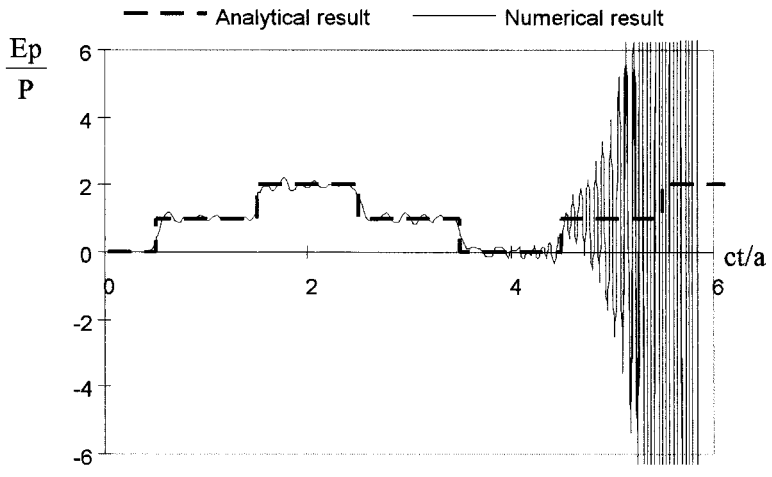

Figure 3. Time histories of the flux at point D($a/2, b/2$) for the waveguide with 128 finite elements and 64 boundary elements: model I, $\theta = 1.0$, and $\beta = 0.6$

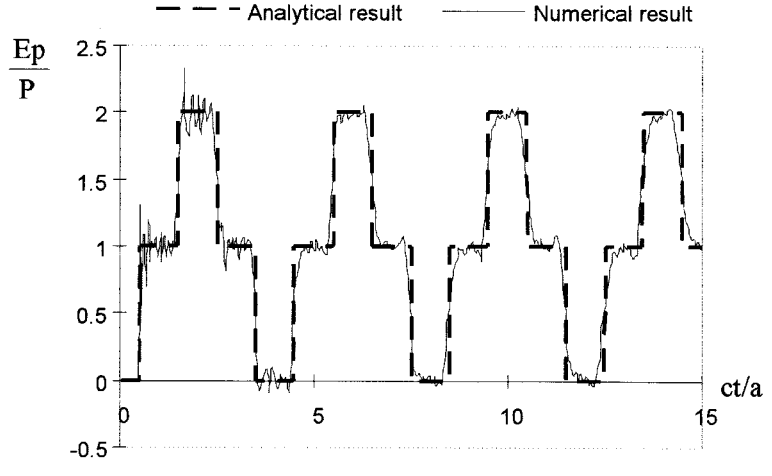

Figure 4. Time histories of the flux at point D($a/2, b/2$) for the waveguide with 128 finite elements and 64 boundary elements: model II, $\theta = 1.4$, and $\beta = 0.6$.

part being modelled by linear BE with the same length l. Linear-time interpolation functions for both potentials and fluxes were adopted in the BE formulation.

In the first analysis, 64 FE and 32 BE (see Figure 2(b)) were used. Subsequently, a second analysis with 128 FE and 64 BE was carried out. The flux time history for this second analysis, referred to here as model I, at the FE and BE meshes interface point D($a/2, b/2$), obtained from the standard time-domain BEM formulation (i.e. $\theta = 1.0$) for $\beta = 0.6$ ($\beta = c\Delta t/l$) is shown in

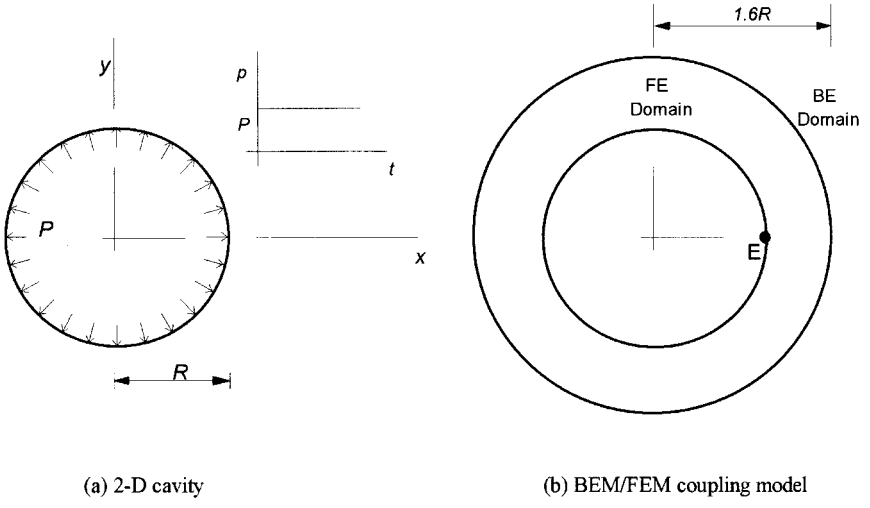

Figure 5. 2-D cavity problem.

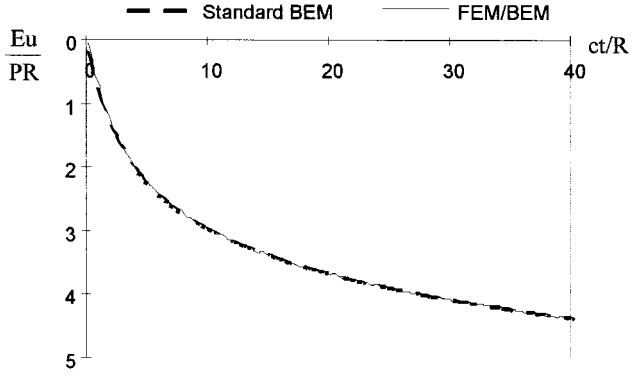

Figure 6. Time histories of displacements at point E(R, 0) for the 2-D cavity problem, for $\beta = 0.6$ and $\theta = 1.4$, with 128 finite elements and 32 boundary elements.

Figure 3, where a quick deterioration of the numerical results can be observed. This behaviour also occurred in the analysis carried out by the authors with the less refined mesh shown in Figure 2(b), and although later, was also observed for potential at point D($a/2$, $b/2$) for both analyses.

Other analyses where the finite element region shown in Figure 2(b) was discretized with boundary elements and *vice versa* were also carried out, and in this case instability started much earlier. This case, referred to here as model II, showed to be more critical than that where model I was employed; thus, it was chosen to verify the improvement of stability achieved by the linear θ approach discussed in this paper. As one can see from Figure 4, a great improvement of stability

was achieved with $\theta = 1.4$. Other analyses, carried out for $1.2 \leqslant \theta \leqslant 2.0$, showed that in this range good results are obtained, and that increasing θ improves stability, but introduces artificial damping in the numerical results.

Two-dimensional cavity

Figure 5 shows a cylindrical (2-D) cavity of radius R in an infinite space. At $t = 0$ a boundary flux p was suddenly applied and kept constant until the end of the analysis. One hundred and twenty-eight triangular finite elements were used in the region from $r = R$ to $1.6R$, whereas 32 boundary elements with the same length l were used at $r = 1.6R$.

Time history of the potential at the boundary point E obtained from the standard BEM/FEM coupling formulation ($\theta = 1.0$) was unstable from $ct/R = 25$ onwards, whereas results obtained with the present approach with $\theta = 1.4$, shown in Figure 6, are stable for the whole time length of the present analysis, i.e. up to $ct/R = 40$. It is important to observe that the instability in this analysis was due to the coupling process, as for this analysis the standard BEM is stable as shown by Yu *et al.* [3].

CONCLUSIONS

A new approach for coupling BEM and FEM in scalar dynamic time-domain analyses has been presented in this paper. The approach used for the BEM algorithm, named linear θ method, permits the use of linear time interpolation functions for boundary fluxes in a coupling procedure where Newmark method is used for the FEM algorithm. The algorithm was described in this paper and used to analyse two examples, one of them prone to numerical instabilities.

The following conclusions can be inferred from the discussion presented here:

1. It is now possible to use linear time interpolation for BEM fluxes in coupling BEM/FEM algorithms for scalar dynamic time-domain analyses.
2. The computer costs of the linear θ method and the classical BEM are very much the same, however stability in closed domain analyses is substantially improved when the former is used. Besides, the linear θ method can be easily implemented into existing BEM/FEM coupling algorithms.
3. As θ increases stability improves; however large values of θ can bring excessive numerical damping into the analysis.

The θ procedure presented here can be easily extended to 3-D acoustics and to 2-D and 3-D elastodynamics time-domain approaches. In fact, results as good as those shown here have already been obtained for 2-D elastodynamics [10].

ACKNOWLEDGEMENTS

The authors would like to acknowledge the support of CNPq (research grants 301104/95-6 (NV) and 300210/92-2 (RN)) and PRONEX/MCT to this research work.

REFERENCES

1. Bathe KJ, Wilson EL. Stability and accuracy analysis of direct integration methods. *Earthquake Engineering Structural Dynamics* 1973; **1**(3):283–291.
2. Bathe KJ. *Finite Element Procedures in Engineering Analysis*. Prentice Hall, Englewood Cliffs, NJ, 1996.
3. Yu G, Mansur WJ, Carrer JAM, Gong L. A linear θ method applied to 2D time-domain BEM. *Communications in Numerical Methods in Engineering* 1998; **14**(12):1171–1179.
4. Manolis GD, Beskos DE. *Boundary Element Methods in Elastodynamics*. Unwin Hyman Publishing Co.: London, 1988.
5. Dominguez J, Gallego R. Time-domain boundary element method for dynamic stress intensity factor computations. *International Journal for Numerical Methods in Engineering* 1992; **33**(3):635–647.
6. Beskos DE. Boundary element methods in dynamic analysis: Part II (1986–1996). *Applied Mechanics Review* 1997; **50**(3):149–197.
7. Mansur WJ. A time-stepping technique to solve wave propagation problems using the boundary element method. *Ph.D. Thesis*, University of Southampton, 1983.
8. Mansur WJ, Carrer JAM, Siqueira EFN. Time discontinuous linear traction approximation in time-domain BEM scalar wave propagation analysis. *International Journal for Numerical Methods in Engineering* 1998; **42**(4):667–683.
9. Mansur WJ, Carrer JAM. Two-dimensional transient BEM analysis for the scalar wave equation: kernels. *Engineering Analysis with Boundary Elements* 1993; **12**(4):283–288.
10. Yu G, Mansur WJ, Carrer JAM. The linear θ method for 2-D elastodynamic BE analysis. *Computational Mechanics* 1999; **24**(2):82–89.

